

Differential Diagnosis of Hepatic Tumors: Value of Contrast-Enhanced Harmonic Sonography Using the Newly Developed Contrast Agent, Sonazoid

Kinuyo Hatanaka^a Masatoshi Kudo^a Yasunori Minami^a Taisuke Ueda^a
Chie Tatsumi^a Satoshi Kitai^a Shunsuke Takahashi^a Tatsuo Inoue^a
Satoru Hagiwara^a Hobyung Chung^a Kazuomi Ueshima^a Kiyoshi Maekawa^b

^aDivision of Gastroenterology and Hepatology, Department of Internal Medicine, and ^bAbdominal Ultrasound Unit, Kinki University School of Medicine, Osaka-Sayama, Japan

Key Words

Contrast-enhanced harmonic ultrasonography · Hepatic tumors · Intranodular hemodynamics · Intratumoral perfusion · Sonazoid · Ultrasonography

Abstract

Objective: To clarify the value of contrast-enhanced harmonic ultrasonography (US) with Sonazoid, a second-generation US contrast agent, in the differential diagnosis of liver tumors compared to dynamic CT. **Methods:** A total of 249 hepatic nodules in 214 patients were studied; these included 177 hepatocellular carcinomas (HCCs), 42 liver metastases, 20 liver hemangiomas, 6 dysplastic nodules and 4 focal nodular hyperplasias (FNHs). After the injection of Sonazoid, nodules were scanned using real-time contrast-enhanced harmonic US in the vascular phases, i.e. the early and late vascular phases, and the Kupffer phase. **Results:** Six enhancement patterns were identified to be significant for the differential diagnosis of hepatic tumors. In HCCs the presence of intratumoral vessels supplied from the periphery and fast wash-out (sensitivity, 96.6%; specificity, 94.4%) were the most typical characteristics. In metastases the presence of rim-like enhancement with peripheral tumor vessels (sensitivity, 88.1%; specificity, 100%) was the typical pattern. In hemangiomas, the presence of intratumoral hypoperfusion images

with globular or cotton wool-like pooling, which continue to the late vascular phase (sensitivity, 90.0%; specificity, 99.6%), was typical. In dysplastic nodules, the presence of portal enhancement without arterial supply in the early vascular phase and the presence of intratumoral uptake in the Kupffer phase (sensitivity, 83.3%; specificity, 100%) were the most typical patterns. In FNHs, the presence of a spoke-wheel pattern in the early vascular phase with dense staining in the late vascular phase, and positive uptake within the nodule in the Kupffer phase (sensitivity, 100%; specificity, 100%) were the most typical patterns. **Conclusion:** Contrast-enhanced harmonic US with Sonazoid allowed intimate vascular and Kupffer imaging and, therefore, is useful for the differential diagnosis of hepatic tumors. Copyright © 2008 S. Karger AG, Basel

Introduction

The evaluation of intranodular hemodynamics is important for the diagnosis of hepatic malignancies because the pathological findings of hepatic malignancies are closely related to intranodular hemodynamics. B-mode ultrasonography (US) is useful for the screening of liver diseases but cannot demonstrate tumor vascularity. Color Doppler imaging reveals the arterial pulsating flows such

KARGER

Fax +41 61 306 12 34
E-Mail karger@karger.ch
www.karger.com

© 2008 S. Karger AG, Basel
0300-5526/08/0517-0061\$24.50/0

Accessible online at:
www.karger.com/int

Masatoshi Kudo, MD, PhD
Division of Gastroenterology and Hepatology, Department of Internal Medicine
Kinki University School of Medicine, 377-2 Ohno-Higashi
Osaka-Sayama 589-8511 (Japan)
Tel. +81 72 366 0221, Fax +81 72 367 2880, E-Mail m-kudo@med.kindai.ac.jp

as a basket pattern flow and a 'spot' pattern flow for hepatic tumor differentiation [1, 2]. However, color Doppler US does not detect pulsatile flow in some hepatocellular carcinomas (HCCs). The reasons for this are as follows. First, color Doppler US cannot detect flows that are perpendicular to the sound field [3]. Second, the technique uses an estimate of the mean Doppler frequency shift at a particular position. On the contrary, power Doppler imaging measures the Doppler energy, which is based on the integrated power of the Doppler signal instead of its mean Doppler frequency shift. Some studies reported that power Doppler sonography was more sensitive for the depiction of blood vessels than color Doppler imaging [3, 4]. These techniques are noninvasive and inexpensive; however, they have some limitations including a low sensitivity of detecting the microflow in the nodules.

Efforts have been made to improve both sonography instruments and contrast agents to detect flow in tumors with more sensitivity [5, 6]. Sonography with an intraarterial CO₂ microbubble contrast agent enabled the detection of intratumoral hemodynamics, and the differential diagnosis of hepatic tumors has become possible with contrast-enhanced harmonic US from the information obtained from tumor vascularity [7]. Contrast-enhanced US using Levovist involved the use of the non-linear backscatter property of the resonant microbubbles produced by an intravenously administered contrast agent; it allows microflow imaging of nodules and eliminates clutter signals. However, Levovist bubbles easily collapse by US emission because of its fragile property. Therefore, Levovist-enhanced harmonic US images are basically obtained intermittently, and real-time images are obtained within a short period of time at an early vascular phase, and Kupffer imaging in the post-vascular phase can be performed by a single sweep scan of the liver.

With the development of the second-generation contrast media such as Sonazoid, which are made of a hard shell containing bubbles within them, contrast-enhanced harmonic US has entered a new era. Sonazoid produces stable non-linear oscillations in the low-power acoustic field (i.e. low mechanical index), and supplies great details of the second harmonic signals in real time. This contrast agent provides detailed perfusion features of the microvascular bed of the liver parenchyma and tumor during the vascular phase. Moreover, Kupffer imaging in the post-vascular phase, which is stable for at least up to 3 h after injection and tolerable for multiple scanning, can be obtained in the low-power acoustic field because Sonazoid microbubbles are phagocytosed by Kupffer cells [8].

The purpose of this study was to assess the value of contrast-enhanced harmonic US using Sonazoid for the differential diagnosis of liver tumors.

Patients and Methods

The Ethics Committee of our institution approved the study protocol. Written informed consent was obtained from all patients at enrollment.

Patients

Between January 2007 and August 2007, 251 consecutive patients with 382 liver tumors detected on screening US were assessed with contrast-enhanced US using Sonazoid. Of the 382 hepatic tumors, 133 pretreated hepatic tumors were excluded. No other exclusion criteria were considered. Thus, 214 patients with 249 liver tumors were included in this study: 134 men and 80 women, ranging in age from 32 to 83 years (mean \pm SD, 68 \pm 9.6 years).

The final diagnoses of the hepatic tumors were HCC in 177 nodules, liver metastasis in 42 nodules (14 from colon cancer, 6 from pancreatic cancer, 5 from gastric cancer, 5 from cholangiocellular carcinoma, 3 from gallbladder cancer, 2 from uterine cancer, 2 from ovarian cancer, 1 from breast cancer, 1 from acute myeloid leukemia, 1 from renal cancer, 1 from lung cancer and 1 melanoma), hemangioma in 20, dysplastic nodule in 6 and focal nodule hyperplasia (FNH) in 4. Intranodular vascularity was evaluated in the 249 nodules.

The maximal diameters of the 249 hepatic nodules were as follows: HCCs, 6–100 mm (mean \pm SD, 22.6 \pm 16.3 mm); metastases, 5–96 mm (mean \pm SD, 33.6 \pm 24.4 mm); hemangiomas, 7–180 mm (mean \pm SD, 29.4 mm \pm 40.3); dysplastic nodules, 10–19 mm (mean \pm SD, 13.5 \pm 3.6 mm), and FNH, 20–35 mm (mean \pm SD, 23.0 \pm 8.1 mm). Histological diagnosis was obtained following sonographically guided percutaneous biopsy or surgery in 9 HCCs, 4 metastases, 2 hemangiomas, 6 dysplastic nodules and 4 FNHs. The other 226 nodules were diagnosed on the basis of tumor markers and a combination of imaging findings such as contrast-enhanced CT, superparamagnetic iron oxide-enhanced MRI, and/or CT hepatic angiography and arterial portography [9], and patients were followed up $>$ 6 months.

Multidetector raw CT with a 64-channel (Aquilion; Toshiba, Tokyo, Japan) was used for diagnosis. In addition to plain CT, triple-phase contrast-enhanced CT scans were performed 30, 60 and 180 s after the initiation of the injection of the contrast medium with a 5.0-mm slice thickness, to obtain hepatic arterial, portal venous and equilibrium phase images, respectively. A total of 100 ml of non-ionic contrast material containing 300 mg iodine/ml (iomeprol; Eisai, Tokyo, Japan) was injected intravenously at a rate of 3 ml/s using an automatic power injector.

US Contrast Medium

Sonazoid (Daiichi-Sankyo, Tokyo, Japan; GE Healthcare, Milwaukee, Wisc., USA) is a second-generation microbubble agent of US. Sonazoid consists of perfluorobutane microbubbles with a median diameter of 2–3 μ m [10]. It was reconstituted with 2 ml sterile water for injection. The recommended clinical dose for the imaging of liver lesions is 0.015 ml encapsulated gas per kilogram

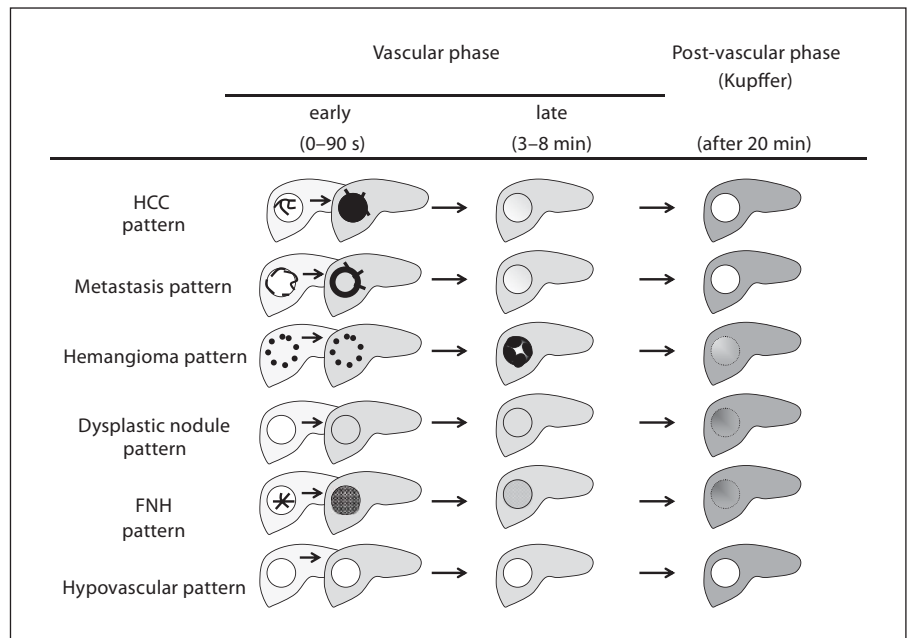


Fig. 1. Diagram of the intranodular hemodynamic patterns of hepatic tumors in the early, late and post-vascular phases.

body weight. Sonazoid was injected as a bolus at a speed of 1 ml/s via a 22-gauge cannula placed in the antecubital vein, and flushed with 10 ml normal saline. Diluted formulations were used within 1 h of reconstitution.

Imaging

To minimize variation between operators, the contrast-enhanced harmonic US studies were performed by either of two operators (K.H. and K.M.) using the same examination protocol.

The B-mode sonographic scans were obtained using a GE LOGIQ 7 (GE Medical Systems, Milwaukee, Wisc., USA) with a 4-MHz convex transducer or a 6.5-MHz transducer. The acoustic power of contrast-enhanced US was set at the default settings with a mechanical index of 0.2; the dynamic range was fixed at 60–65 dB. A single focus point was set 10 cm deep.

After injection of Sonazoid, when the first microbubble signal appeared in the liver parenchyma, the patient was requested to hold his/her breath. The images of the ideal scanning plane were displayed in real-time mode for all phases. The vascular findings on phase-inversion harmonic sonography were shown as tumor vessel flow in the early vascular phase (about 15–40 s after the injection of Sonazoid). The real-time replenishing images were obtained during the early vascular phase (<2 min after the injection of Sonazoid) by release burst imaging, a method combining multiple high-frequency and broadband detection pulses with a separate release burst. Parenchymal findings were obtained as Kupffer imaging in the post-vascular phase at least 10 min after the intravenous injection of Sonazoid.

Statistical Analysis

The images were stored as a cine clip with GE exclusive raw-data format files in a LOGIQ 7 computer. The cine clip images of B-mode and contrast-enhanced US were played back, and at least three observers evaluated the intratumoral hemodynamics and

classified them into seven patterns without knowing the pathologic or clinical data. When there were discrepancies, the cine clips were discussed and reassessment was performed to reach agreement. The intratumoral vascularity on contrast-enhanced US was assessed as hyperperfusion, isoperfusion or hypoperfusion by comparing the staining patterns of the intratumoral vessels and parenchyma with those of the surrounding liver parenchyma. The enhancement patterns in each phase were evaluated.

The indication of hyperperfusion and isoperfusion was defined as a positive depiction of intratumoral vascularity. Data were expressed as means \pm SD. Differences in clinical characteristics between the two groups were compared using the χ^2 and unpaired t tests. $p < 0.05$ was considered significant.

Results

Enhancement Patterns

Of the 216 patients, 158 showed liver cirrhosis or chronic hepatitis. Of the 177 HCCs in 147 patients, 118 were hypoechoic, 28 had a mosaic pattern, 22 were hyperechoic and 9 had isoechoic lesions on B-mode sonography. Of the 42 metastases, 17 were hypoechoic, 8 had cluster characteristics, 7 had a bull's eye pattern, 5 were hyperechoic and 5 had isoechoic lesions on B-mode sonography.

The intranodular hemodynamic patterns of the nodular hepatic lesions were classified as follows (fig. 1): pattern 1 (HCC pattern), abundant tumor vessels appeared as a basket-like or irregular branching image from the

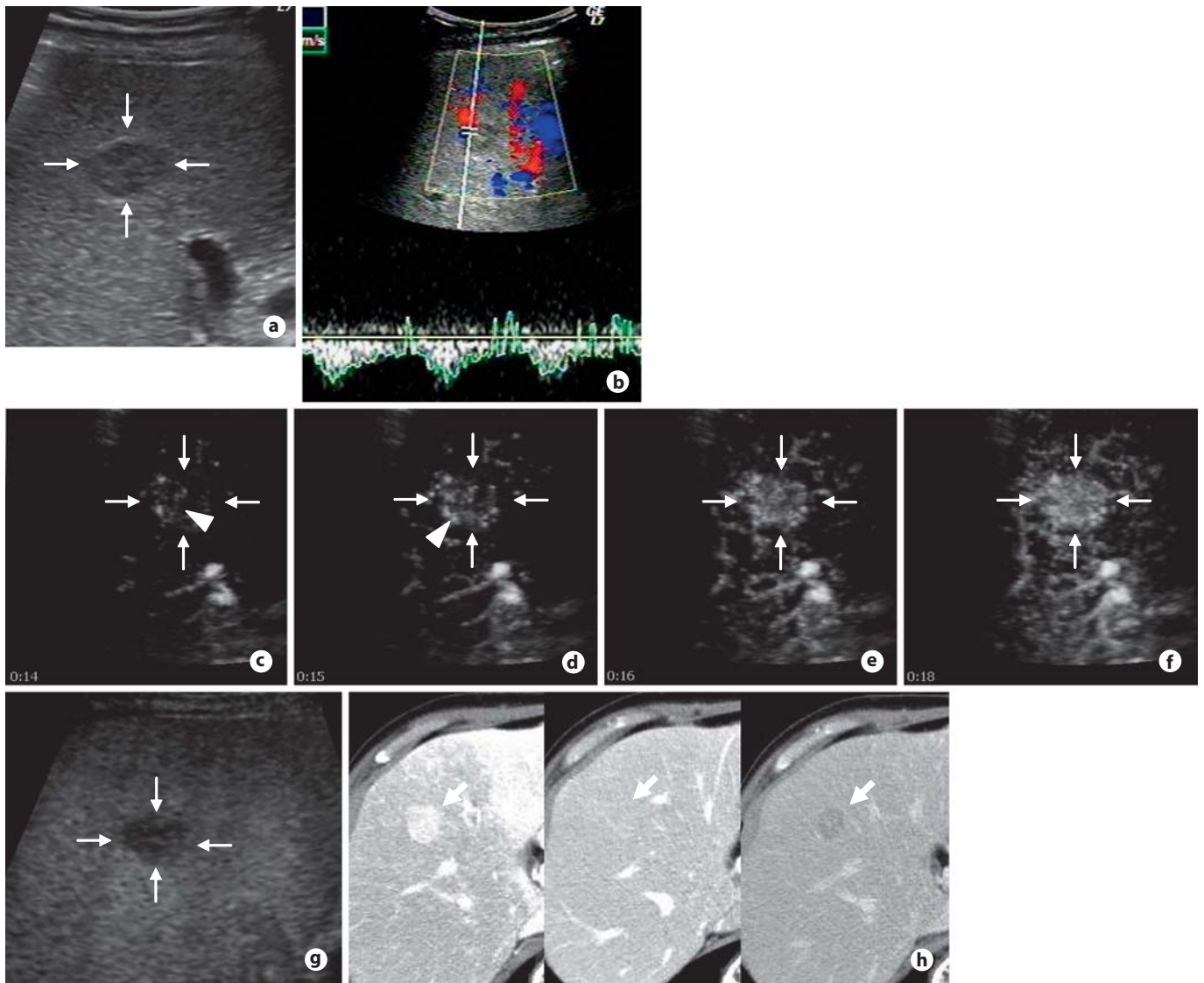


Fig. 2. HCC. **a** B-mode US revealing the hypoechoic nodule (arrows). **b** Color Doppler US showing the hepatic tumor with retrograde constant flow accompanying pulsatile blood flow. **c, d** On contrast-enhanced US, intratumoral vessels (arrowheads) are shown within the tumor (arrows) in the early vascular phase.

e, f Contrast-enhanced US reveals tumor parenchymal staining (arrows) in the vascular phase. **g** Contrast-enhanced US shows the tumor (arrows) as a defect on the gray-scale background in the Kupffer phase. **h** The tumor is shown as a hypervascular mass (arrows) with a fast washout on dynamic CT.

periphery penetrating the center, followed by dense tumor staining in the early vascular phase and fast washout in the late vascular phase with complete Kupffer defect; pattern 2 (metastasis pattern), straight tumor vessels in the marginal and central areas with peripheral parenchymal staining or rim-like enhancement with complete Kupffer defects in the post-vascular phase; pattern 3 (hemangioma pattern), globular pooling or a cotton wool-like imaging with a gradual fill-in over time that continued until 5 or 10 min; pattern 4 (dysplastic nodule

pattern), no tumor vessel and portal perfusion without arterial perfusion with real-time scanning in the early vascular phase and no apparent Kupffer defect; pattern 5 (FNH pattern), centrifugal spoke-wheel arterial supply with continuing dense parenchymal staining in the vascular phase with no Kupffer defect; pattern 6 (atypical pattern), various tumor vessels and various parenchymal perfusions from those described above, and pattern 7 (hypovascular pattern), no tumor vessel and no parenchymal perfusion in all phases.

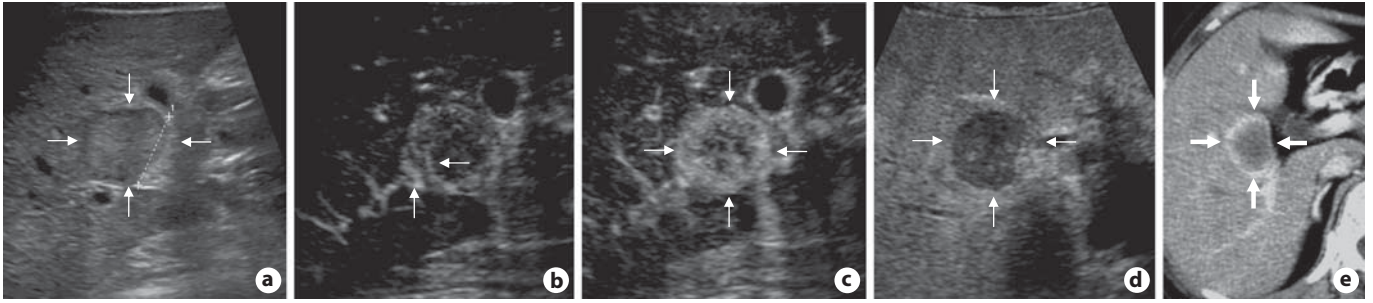


Fig. 3. Metastasis. **a** B-mode US shows the hepatic tumor (arrows) with a bull's eye pattern. **b** Contrast-enhanced US shows intratumoral and peritumoral linear vessels (arrows) in the early vascular phase. **c** Contrast-enhanced US shows rim-like enhancement (arrows) in the vascular phase. **d** Contrast-enhanced US shows the tumor (arrows) as a defect on the gray-scale background in the Kupffer phase. **e** The tumor is shown as a rim-like enhancement (arrows) on dynamic CT.

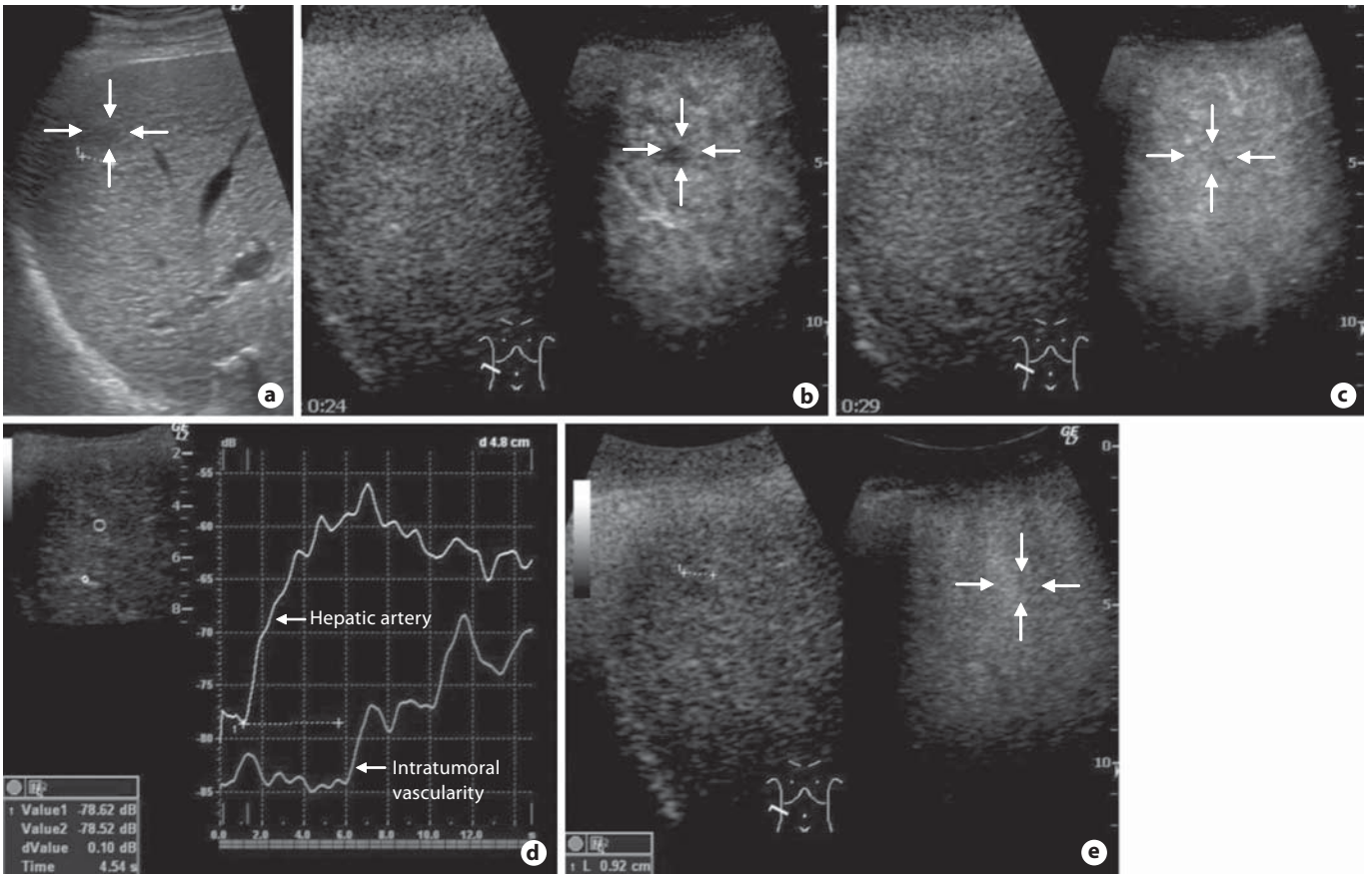


Fig. 4. Dysplastic nodule. **a** B-mode US shows the hypochoic nodule (arrows). **b** Contrast-enhanced US shows no blood signal within the hypochoic nodule (arrows) in the early vascular phase. **c** After 5 s, contrast-enhanced US shows isoperfusion with the gray-scale background (arrows). **d** On the time intensity curve, contrast-enhanced US clearly shows the tumor with no arterial vascularity and portal flow. **e** The tumor reveals isoperfusion (arrows) on the gray-scale background in the Kupffer phase.

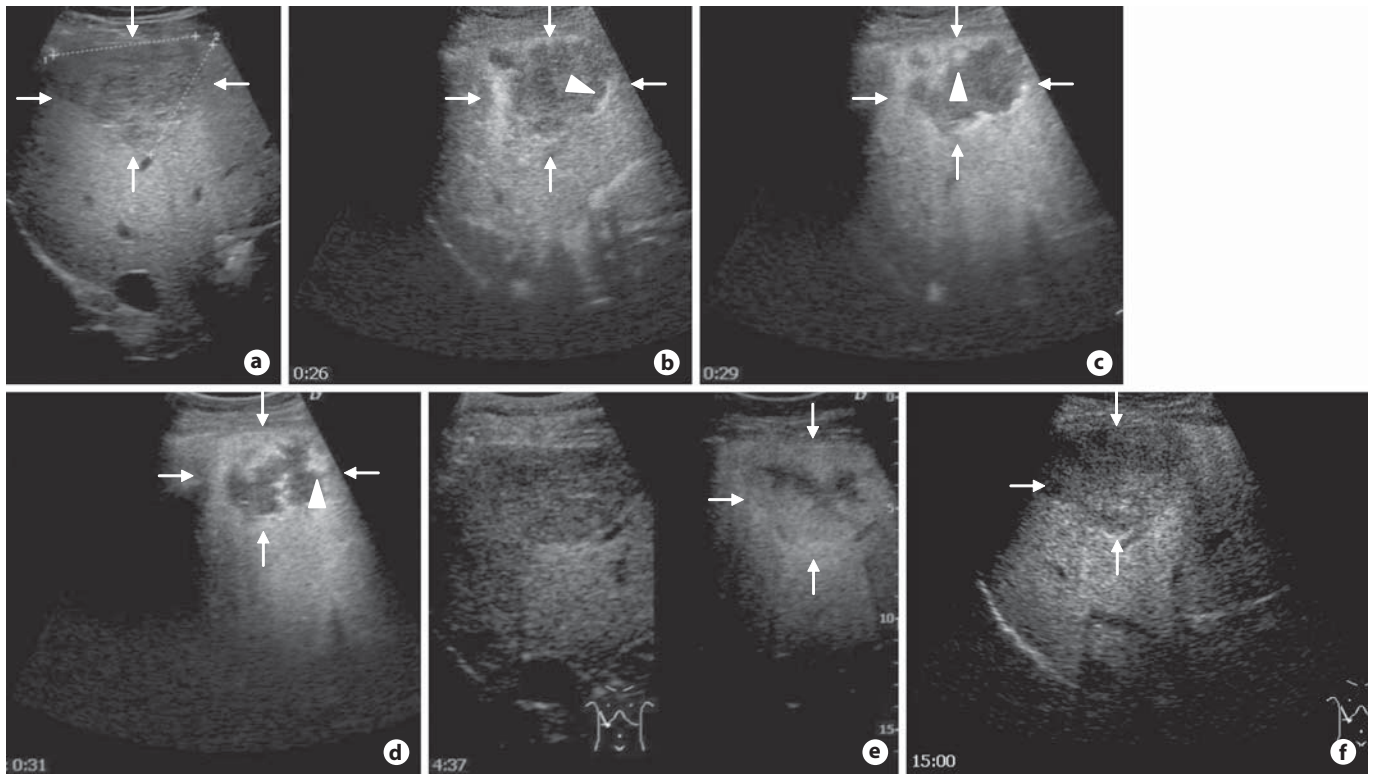


Fig. 5. Hemangioma. **a** B-mode US shows the hypoechoic nodule (arrows). **b** Contrast-enhanced US shows peripheral spotty pooling (arrowhead) within the nodule (arrows) in the early vascular phase. **c, d** Contrast-enhanced US shows typical globular tumor parenchymal staining (arrowheads) within the nodule (arrows) in

the late vascular phase. **e** Gradual fill-in persisted until the late vascular phase within the nodule (arrow). **f** The tumor is shown as iso- or hypoperfusion (arrows) on the gray-scale background in the Kupffer phase.

Hepatocellular Carcinoma

Intranodular vascularity was detected in 99.4% (176/177) of HCCs on contrast-enhanced harmonic US. In the remaining 0.6% (1/177) of HCCs, no blood signal was detected. In contrast, 98.9% (175/177) of HCCs showed hyper- or isoperfusion on dynamic CT.

Of 176 HCCs, a total of 171 (97.2%) were classified as pattern 1 (HCC perfusion pattern; fig. 1, 2) on contrast-enhanced harmonic US, 2.3% (4/176) of HCCs were classified as the atypical perfusion pattern (pattern 6) and 0.6% (1/176) of HCCs showed the hypoperfusion pattern (pattern 7). Twenty of 171 HCCs (11.7%) depicting pattern 1 perfusion nodules had small tumor vessels; however, dense intranodular perfusion was present, followed by fast wash-out in the late vascular phase. Sixty-nine of 171 (40.3%) pattern 1 HCCs showed moderate tumor vessels while 48.0% (82/171) of pattern 1 HCCs showed abundant tumor vessels in the early vascular phase on contrast-enhanced harmonic US. In 2.3% of pattern 1 HCCs (4/171), tumor

parenchymal staining was detected only in parts of the nodule. Of the 171 pattern 1 perfusion-type HCCs, 2.3% (4/171) showed partial perfusion defects and 97.7% (147/171) showed entire perfusion defects in the Kupffer phase.

Most of the HCCs showed HCC perfusion patterns on contrast-enhanced harmonic US. The sensitivity and specificity of the hepatocellular carcinoma pattern were 96.6 (171/177) and 94.4% (68/72), respectively. The positive and negative predictive values of this pattern were 97.7 (171/175) and 91.9% (68/74), respectively.

Metastasis

In 37 nodules of 42 metastases, contrast-enhanced US showed linear tumor vessels and marginal rim-like parenchymal staining. Although the other 5 metastases had small tumor vessels and weak parenchymal perfusion, all metastases showed clear Kupffer defects in the post-vascular phase. Most of the metastases showed a type 2 perfusion pattern (fig. 1, 3) on contrast-enhanced US. The

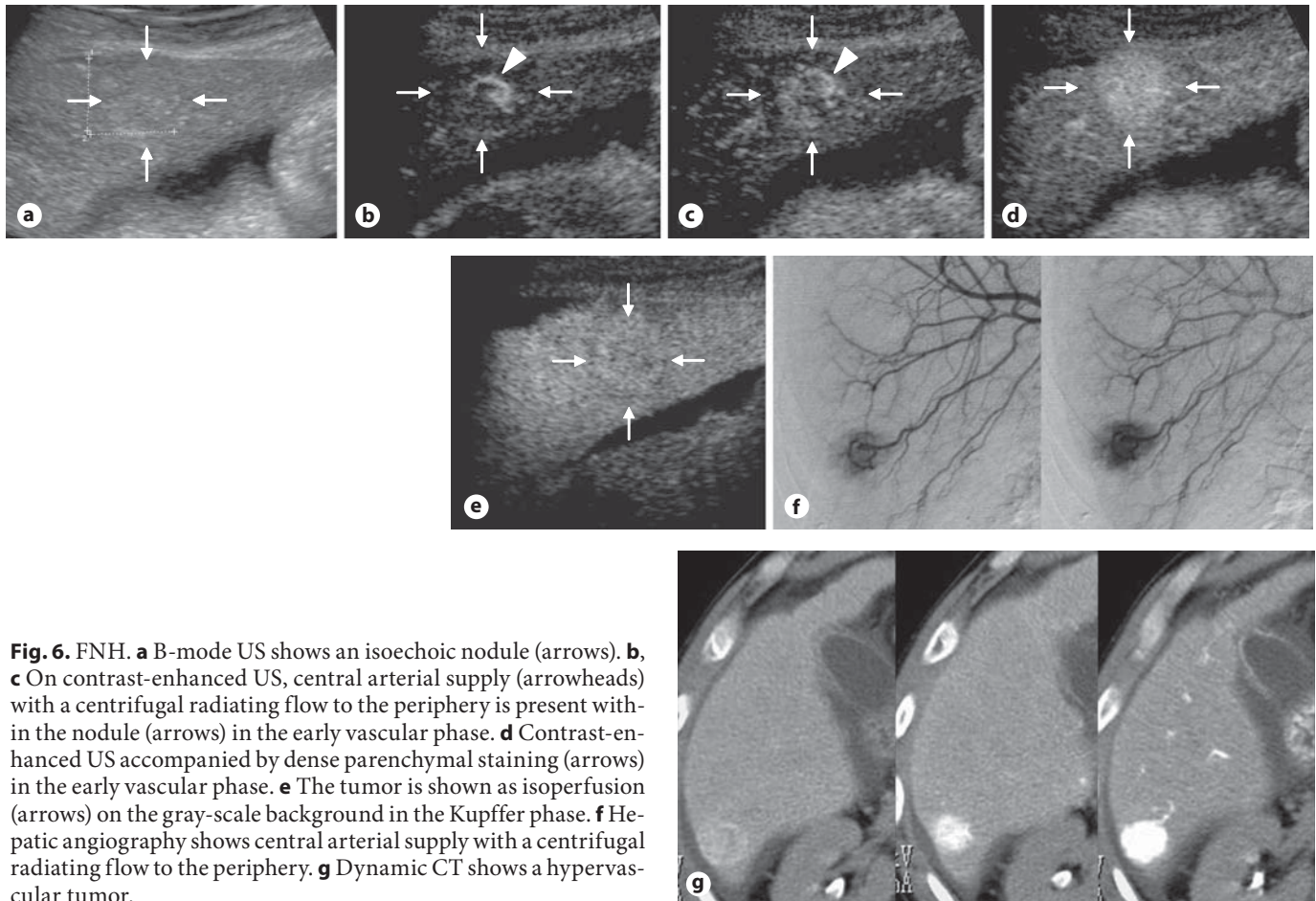


Fig. 6. FNH. **a** B-mode US shows an isoechoic nodule (arrows). **b**, **c** On contrast-enhanced US, central arterial supply (arrowheads) with a centrifugal radiating flow to the periphery is present within the nodule (arrows) in the early vascular phase. **d** Contrast-enhanced US accompanied by dense parenchymal staining (arrows) in the early vascular phase. **e** The tumor is shown as isoperfusion (arrows) on the gray-scale background in the Kupffer phase. **f** Hepatic angiography shows central arterial supply with a centrifugal radiating flow to the periphery. **g** Dynamic CT shows a hypervascular tumor.

sensitivity and specificity of the metastasis pattern were 88.1 (37/42) and 100% (207/207), respectively. The positive and negative predictive values of this pattern were 100 (37/37) and 97.6% (207/212), respectively.

Hemangioma

On contrast-enhanced harmonic US, all hemangiomas revealed hypervascularity, and pattern 3 perfusion (fig. 1, 4) hemangiomas were present in 18 nodules. Gradual fill-in and globular parenchymal enhancement in the late vascular phase persisted until the post-vascular phase. The sensitivity and specificity of the hemangioma pattern were 90.0 (18/20) and 99.6% (228/229), respectively. The positive and negative predictive values of this pattern were 94.7 (18/19) and 99.1% (228/230), respectively. Two hemangiomas showed tumor vessels and dense parenchymal pooling in the early vascular phase, which was difficult to distinguish from the hemodynamic pattern of HCC. However, the intranodular pooling contin-

ued to the late vascular phase, leading to a correct diagnosis of hemangioma.

Dysplastic Nodules

Contrast-enhanced US showed no tumor vessels and portal perfusion without arterial perfusion in all of the 5 dysplastic nodules in the early vascular phase. In the late vascular and post-vascular phases, contrast-enhanced harmonic US showed isoperfusion in 4 tumors and hyperperfusion in 1 tumor. The remaining nodule showed no tumor vessel and hypovascular perfusion in the three phases. The sensitivity and specificity of pattern 4 (fig. 1, 5) were 83.3 (5/6) and 100% (244/244), respectively. The positive and negative predictive values of this pattern were 100 (5/5) and 99.6% (244/245), respectively.

Focal Nodular Hyperplasia

All 4 FNHs showed a central arterial supply with a centrifugal radiating flow to the periphery (spoke-wheel

pattern) and dense parenchymal staining in the late vascular phase (type 5) with no Kupffer defect (fig. 1, 6). The sensitivity and specificity of the FNH pattern were 100 (4/4) and 100% (4/4), respectively. On dynamic CT, the spoke-wheel pattern was not detected in any of the 4 FNHs, and only hyperperfusion was observed.

Discussion

Various gases or shells have been studied for their use as sonographic contrast agents [8–11], and contrast-enhanced harmonic US using various media has been possible [6, 12–14]. Sonazoid has been licensed from January 2007 exclusively in Japan. Gas carrier contrast agents consist of microbubbles that are small enough to pass through the pulmonary circulation, and these microbubbles are sufficiently stable to pressure to circulate through the left ventricle after intravenous administration. Because Sonazoid microbubbles are phagocytosed by Kupffer cells, and Kupffer imaging, which is extremely stable and tolerable for multiple scanning at least up to 180 min, in the post-vascular phase, is feasible. Once Sonazoid is administered to the patient via a vein, both blood vessel imaging and liver parenchymal imaging (Kupffer imaging) can be obtained. These properties are completely different from SonoVue and Definity.

Levovist-enhanced harmonic US can demonstrate images under high sound pressure, and only intermittent imaging is obtained. However, Sonazoid-enhanced harmonic US demonstrates images under a low acoustic pressure, producing much clearer real-time images. Therefore, it is much easier to scan the intratumoral hemodynamics repeatedly using Sonazoid-enhanced harmonic US.

Compared to dynamic CT, Sonazoid-enhanced US requires no radiation exposure and a smaller amount of contrast agent. Although there is one contraindication for patients who are allergic to eggs, patients with renal dysfunction or iodine-allergic patients can also be examined using this technique unlike CT. Moreover, Sonazoid is taken up by the Kupffer cells, which is different from other contrast agents, and the information of Kupffer function provides essential information compared to other contrast agents [8, 15].

D'Onofrio et al. [14] reported that SonoVue-enhanced US detected hepatic malignancy as defects in the sinusoidal phase with a sensitivity of 85%, specificity of 88%, positive predictive value of 92% and negative predictive value of 77%. In our study, Sonazoid-enhanced harmonic US detected hepatic malignancy as defects on the sinu-

soidal phase with a sensitivity of 95% (208/219), specificity of 93.3% (28/30), positive predictive value of 99% (208/210) and negative predictive value of 97.4% (38/39). These favorable results can be attributed to the beautiful features of Kupffer imaging.

The evaluation of the deeply located nodules was difficult using contrast-enhanced harmonic US using Levovist in previous reports [6, 13, 16]. In this study, 8.4% (21/249) of hepatic tumors were located 10 cm beneath the skin surface. However, contrast-enhanced US with Sonazoid allowed sufficient imaging to evaluate the intratumoral vascularity, which is another favorable point compared to Levovist.

On angiography, CO₂ sonographic angiography and CT arteriography, HCC shows hypervascularity with an arterial supply and dense tumor perfusion [5, 7, 12, 16, 17]. In our study, Sonazoid-enhanced harmonic US showed that 96.6% of HCCs (171/177) have arterial supply from the periphery, homogeneous or heterogeneous dense hyperperfusion, and fast washout with clear Kupffer defect. On contrast-enhanced harmonic US, the formation of homogeneous or heterogeneous staining in the early vascular phase and the formation of washout in the late vascular phase were similar to dynamic CT. Evaluating the perfusion imaging at all three phases may allow to assess the intranodular hemodynamic features of HCCs more precisely.

Using contrast-enhanced harmonic US, 88.1% (37/42) of metastases were shown to have peripheral linear tumor vessels with rim-like enhancement between the non-enhanced portion of the lesion and the enhanced surrounding parenchyma. This perfusion pattern was never seen in other liver tumors, and was similar to the pattern obtained with dynamic CT. All metastases were demonstrated as clear defects in the Kupffer phase. Only 4 nodules of metastasis showed an atypical pattern which might be caused by the different characteristics of the primary cancer.

On contrast-enhanced harmonic US, typical spotty pooling in the vascular phase followed by globular or cotton wool pooling was detected in the hemangiomas. This perfusion pattern was not seen in any other hepatic tumors. Small-sized hemangiomas occasionally showed early tumor vessels and parenchymal perfusion in the vascular phase. However, this intratumoral perfusion continued to the Kupffer phase, leading to the correct diagnosis of hemangioma.

Many studies have described the hemodynamic characteristics of dysplastic nodules as portal supply and arterial hypovascularity [4, 17–19]. In this study, contrast-enhanced US demonstrated 5 dysplastic nodules with ar-

terial hypovascularity and portal supply in the early vascular phase. The positive uptake in the Kupffer phase might also have been attributed to the presence of the Kupffer cells in the nodules. The diagnostic criteria of the dysplastic nodules have a high specificity and positive predictive value but low sensitivity.

Previous studies reported that the spoke-wheel appearance is a pathognomonic finding for FNHs [7, 20]. In this study, all FNHs had the typical arterial supply of the spoke-wheel appearance. The sensitivity and specificity of the FNH pattern were both 100%. Contrast-enhanced harmonic US could directly show the depiction of tumor vessels, this is superior to dynamic CT or Levovist-enhanced US for the diagnosis of FNHs.

There were some limitations in this study. First, the criterion for diagnosis was not applied prospectively. A prospective study is needed to confirm the accuracy for

differential diagnosis of hepatic nodules. Second, the proportion of HCC tumors in our study appeared to be relatively higher than that in Western countries. Another limitation is the preliminary nature of the study, with a relatively small number of patients. Further studies in larger patient cohorts are warranted.

In conclusion, Sonazoid-enhanced harmonic US is a promising technique for the noninvasive characterization of hepatic tumors based on the sensitive and specific presence/absence of the characteristic features of each tumor type.

Disclosure Statement

The authors declare that they have no financial conflict of interest.

References

- 1 Tanaka S, Kitamura T, Fujita M, Nakahashi K, Okuda S: Color Doppler flow imaging of liver tumors. *AJR* 1990;154:509–514.
- 2 Tanaka S, Kitamura T, Fujita M, Kasugai H, Inoue A, Ishiguro S: Small hepatocellular carcinoma: differentiation from adenomatous hyperplastic nodule with color Doppler flow imaging. *Radiology* 1992;182:161–165.
- 3 Rubin JM, Bude RO, Carson PL, Bree RL, Adler RS: Power Doppler US: a potentially useful alternative to mean frequency-based color Doppler US. *Radiology* 1994;190:853–856.
- 4 Koito K, Namieno T, Morita K: Differential diagnosis of small hepatocellular carcinoma and adenomatous hyperplasia with power Doppler sonography. *AJR* 1998;170:157–160.
- 5 Fujimoto M, Moriyasu F, Nishikawa K, Nada T, Okuma M: Color Doppler sonography of hepatic tumors with a galactose-based contrast agent: correlation with angiographic findings. *AJR* 1994;163:1099–1104.
- 6 Ding H, Kudo M, Onda H, Suetomi Y, Minami Y, Maekawa K: Hepatocellular carcinoma: depiction of tumor parenchymal flow with intermittent harmonic power Doppler US during the early arterial phase in dual-display mode. *Radiology* 2001;220:349–356.
- 7 Kudo M, Tomita S, Tochio H, Mimura J, Okabe Y, Kashida H, Hirasa M, Ibuki Y, Todo A: Sonography with intraarterial infusion of carbon dioxide microbubbles (sonographic angiography): value in differential diagnosis of hepatic tumors. *AJR* 1992;158:65–74.
- 8 Yanagisawa K, Moriyasu F, Miyahara T, Yuki M, Iijima H: Phagocytosis of ultrasound contrast agent microbubbles by Kupffer cells. *Ultrasound Med Biol* 2007;33:318–325.
- 9 Kudo M, Okanoue T; Japan Society of Hepatology: Management of hepatocellular carcinoma in Japan: consensus-based clinical practice manual proposed by the Japan Society of Hepatology. *Oncology* 2007;72(suppl 1):2–15.
- 10 Sontum PC, Ostensen J, Dyrstad K, Hoff L: Acoustic properties of NC100100 and their relation with the microbubble size distribution. *Invest Radiol* 1999;34:268–275.
- 11 Maresca G, Summari V, Colagrande C, Manfredi R, Calliada F: New prospects for ultrasound contrast agents. *Eur J Radiol* 1998;27:171–178.
- 12 Kudo M: Morphological diagnosis of hepatocellular carcinoma: special emphasis on intranodular hemodynamic imaging. *Hepato-gastroenterology* 1998;45:1226–1231.
- 13 Isozaki T, Numata K, Kiba T, Hara K, Morimoto M, Sakaguchi T, Sekihara H, Kubota T, Shimada H, Morizane T, Tanaka K: Differential diagnosis of hepatic tumors by using contrast enhancement patterns at US. *Radiology* 2003;229:798–805.
- 14 D'Onofrio M, Martone E, Faccioli N, Zamboni G, Malagò R, Mucelli RP: Focal liver lesions: sinusoidal phase of CEUS. *Abdom Imaging* 2006;31:529–536.
- 15 Watanabe R, Matsumura M, Chen CJ, Kaneda Y, Fujimaki M: Characterization of tumor imaging with microbubble-based ultrasound contrast agent, Sonazoid, in rabbit liver. *Biol Pharm Bull* 2005;28:972–977.
- 16 Wang J-H, Lu S-N, Hung C-H, Chen TY, Chen CH, Changchien CS, Lee CM: Small hepatic nodules (≤ 2 cm) in cirrhosis patients: characterization with contrast-enhanced ultrasonography. *Liver Int* 2006;6:928–934.
- 17 Matsui O, Kadoya M, Kameyama T, Yoshikawa J, Takashima T, Nakanuma Y, Unoura M, Kobayashi K, Izumi R, Ida M, Kitagawa K: Benign and malignant nodules in cirrhotic livers: distinction based on blood supply. *Radiology* 1991;178:493–497.
- 18 Takayama T, Makuuchi M, Hirohashi S, Sakamoto M, Okazaki N, Takayasu K, Kosuge T, Motoo Y, Yamazaki S, Hasegawa H: Malignant transformation of adenomatous hyperplasia to hepatocellular carcinoma. *Lancet* 1990;336:1150–1153.
- 19 Mathieu D, Bruneton JN, Drouillard J, Pointréau CC, Vasile N: Hepatic adenomas and focal nodular hyperplasia: dynamic CT study. *Radiology* 1986;160:53–58.
- 20 Wanless IR, Mawdsley C, Adams R: On the pathogenesis of focal nodular hyperplasia of the liver. *Hepatology* 1985;5:1194–1200.